ARTICLE
Journal of Cellular Biochemistry 108:1102–1116 (2009)

Journal of Cellular Biochemistry

Physiological and Coordinate Downregulation of the NPC1 and NPC2 Genes Are Associated With the Sequestration of LDL-Derived Cholesterol Within Endocytic Compartments

David Jelinek,[1] Sarah Mount Patrick,[1] Khameeka N. Kitt,[2] Teddy Chan,[3] Gordon A. Francis,[3] and William S. Garver[1*]

[1]*Department of Pediatrics, The University of Arizona, 1501 N. Campbell Avenue, Tucson, Arizona 85724-5037*

[2]*Department of Cellular Biology and Anatomy, The University of Arizona, 1501 N. Campbell Avenue, Tucson, Arizona 85724-5044*

[3]*Department of Medicine, The James Hogg iCAPTURE Centre for Cardiovascular and Pulmonary Research, University of British Columbia, 1081 Burrard Street, Vancouver, British Columbia, Canada V6Z 1Y6*

ABSTRACT

The Niemann-Pick C1 and C2 (NPC1 and NPC2) proteins have a central role in regulating the transport of lipoprotein-derived cholesterol from endocytic compartments to the endoplasmic reticulum for esterification by acyl-CoA:cholesterol acyltransferase (ACAT) and feedback inhibition of the sterol regulatory element-binding protein (SREBP) pathway. Since the NPC1 gene/protein has recently been shown to be downregulated by feedback inhibition of the SREBP pathway, the present study was performed to determine whether physiological downregulation of the NPC1 gene/protein alters the transport and metabolism of low-density lipoprotein (LDL)-derived cholesterol in human fibroblasts. To perform this study, three different culture conditions were used that included fibroblasts grown in lipoprotein-deficient serum (LPDS), LPDS supplemented with LDL, and LPDS supplemented with LDL, followed by equilibration in the absence of LDL to allow the transport of LDL-derived cholesterol from endocytic compartments and equilibration of cellular sterol pools. The results from this study indicated that in addition to the NPC1 gene/protein, the NPC2 gene/protein was also downregulated by LDL-derived cholesterol-dependent feedback inhibition and that downregulation of both the NPC1 and NPC2 genes/proteins was associated with the sequestration of LDL-derived cholesterol within endocytic compartments, including late endosomes/lysosomes after equilibration. Therefore, it is proposed that physiological and coordinate downregulation of the NPC1 and NPC2 genes/proteins promotes the sequestration of LDL-derived cholesterol within endocytic compartments and serves a role in maintaining intracellular cholesterol homeostasis. J. Cell. Biochem. 108: 1102–1116, 2009.

KEY WORDS: ACAT-ACCESSIBLE POOL; CHOLESTEROL; CHOLESTERYL ESTER; EARLY ENDOSOMES; FIBROBLASTS; LATE ENDOSOMES/LYSOSOMES; LOW-DENSITY LIPOPROTEIN; NIEMANN-PICK TYPE C; STEROL REGULATORY POOL

Cholesterol serves as a structural component of mammalian cell membranes and lipoproteins, a precursor for bile acids, oxysterols, and steroid hormones, and also as a cell-signaling molecule involved in regulating gene expression. Most cells and tissues are fully capable of obtaining cholesterol through de novo cholesterol biosynthesis, in addition to the endocytosis of lipoproteins through the coated-pit pathway. The endocytosis of low-density lipoprotein (LDL) and subsequent transport of LDL-derived cholesterol through cellular compartments is required for maintaining intracellular and whole-body cholesterol homeostasis, and therefore remains a subject of intense investigation.

Studies performed using human fibroblasts have demonstrated that LDL particles bind to LDL receptors (LDLR) and LDL-related protein receptors (LRPR) present on the cell surface that are internalized into endocytic compartments of the cell [Brown and Goldstein, 1986]. It is within distinct acidic compartments, residing between early and late endosomes and to a lesser extent late endosomes/lysosomes, that the bulk of cholesteryl ester contained

Grant sponsor: National Institutes of Health; Grant number: R21-DK071544; Grant sponsor: Canadian Institutes of Health; Grant number: MOP-79532.

*Correspondence to: Dr. William S. Garver, Department of Pediatrics, The University of Arizona, 1501 N. Campbell Avenue, Tucson, AZ 85724-5037. E-mail: wgarver@peds.arizona.edu

Received 1 April 2009; Accepted 7 August 2009 • DOI 10.1002/jcb.22339 • © 2009 Wiley-Liss, Inc.
Published online 10 September 2009 in Wiley InterScience (www.interscience.wiley.com).

within the hydrophobic core of LDL particles is hydrolyzed by an acid lipase to generate LDL-derived cholesterol [Sugii et al., 2003]. Recent identification of both the Niemann-Pick C1 (NPC1) and Niemann-Pick C2 (NPC2) genes, in addition to partial functional characterization of the encoded NPC1 and NPC2 proteins, has revealed that these two proteins have a key role in regulating the transport of LDL-derived cholesterol from endocytic compartments to the endoplasmic reticulum and maintaining intracellular cholesterol homoestasis [Carstea et al., 1997; Naureckiene et al., 2000].

The human NPC1 protein consists of 1,278 amino acids with 13 predicted membrane-spanning domains, five of which represent a conserved sterol-sensing domain that has been shown to bind cholesterol [Ohgami et al., 2004; Liu et al., 2009]. Interestingly, a second and separate domain associated with the NPC1 protein, represented by the conserved N-terminal domain (NTD), has also been shown to bind both cholesterol and oxysterol [Infante et al., 2008a,b]. In contrast, the human NPC2 protein consists of only 132 amino acids with three conserved structural motifs, which include a cysteine-rich region, an N-linked glycosylation site, and a unique proline-rich region [Nakamura et al., 2000]. However, similar to the NPC1 protein, the NPC2 protein is capable of binding cholesterol [Friedland et al., 2003; Ko et al., 2003]. Studies have demonstrated that the NPC2 protein, which resides within the lumen of late endosomes/lysosomes, facilitates the transport of LDL-derived cholesterol to the limiting membrane and functions in a non-redundant cooperative manner with the NPC1 protein to promote the removal of cholesterol from these compartments [Sleat et al., 2004; Cheruku et al., 2006; Infante et al., 2008c].

Although undefined, studies have revealed that the NPC1 protein is associated with a unique late endosome-like compartment referred to as the NPC1-compartment, that transiently interacts with late endosomes/lysosomes to regulate the transport of LDL-derived cholesterol to other cellular compartments, in particular the Golgi apparatus, plasma membrane, and endoplasmic reticulum [Underwood et al., 1998; Neufeld et al., 1999; Garver et al., 2000; Wojtanik and Liscum, 2003]. Early studies that were performed before identification of the NPC1 gene/protein suggested that LDL-derived cholesterol was rapidly transported from endocytic compartments to the plasma membrane, and that only after reaching a critical threshold level in the plasma membrane was cholesterol transported to the endoplasmic reticulum for esterification by acyl-CoA:cholesterol acyltransferase (ACAT) [Brasaemle and Attie, 1990; Lange et al., 1999]. However, later studies indicated that at least a portion (approximately 30%) of the LDL-derived cholesterol derived from endocytic compartments was transported directly to the endoplasmic reticulum, independent of the plasma membrane [Neufeld et al., 1996; Underwood et al., 1998]. Consistent with these results, evidence now indicates that the NPC1 protein specifically regulates the transport of LDL-derived cholesterol to the *trans*-Golgi network using a vesicular-mediated SNARE protein complex, before the cholesterol is then distributed to either the plasma membrane or endoplasmic reticulum [Garver et al., 2002; Urano et al., 2008].

A sterol regulatory pool associated with an undefined region of the endoplasmic reticulum and accessible to both cholesterol and oxysterols is responsible for regulating intracellular cholesterol and lipid homeostasis through the sterol regulatory element-binding protein (SREBP) pathway [Brown and Goldstein, 1997]. The relative amounts of cholesterol and oxysterol modulates function of the SREBP cleavage-activating protein (SCAP) and insulin-induced gene (INSIG-1 and INSIG-2) proteins, respectively, to then modulate translocation and proteolytic processing of membrane-bound transcription factors referred to as SREBP-1 and SREBP-2 [Yabe et al., 2002; Yang et al., 2002]. In brief, when an excess amount of cholesterol and oxysterol are accessible to the sterol regulatory pool, a complex consisting of the INSIG:SCAP:SREBP proteins is formed and retained at the endoplasmic reticulum [Radhakrishnan et al., 2004, 2007]. However, when the amount of cholesterol and oxysterol accessible to the sterol regulatory pool is reduced, affinity between the INSIG and SCAP proteins is lessened, thereby allowing translocation of the SCAP:SREBP complex to the Golgi apparatus for protease-mediated processing of the precursor SREBP proteins that translocate to the nucleus and serve as transcription factors [Nohturfft et al., 2000].

Recent studies have demonstrated that the NPC1 gene/protein are downregulated by LDL-derived cholesterol-dependent feedback inhibition of the SREBP pathway [Garver et al., 2008; Gevry et al., 2008]. As a logical extension of this finding, the present study was performed to determine whether physiological downregulation of the NPC1 gene/protein is associated with the sequestration of LDL-derived cholesterol within endocytic compartments. In brief, the results indicated that in addition to the NPC1 gene/protein, the NPC2 gene/protein was also downregulated by LDL-derived cholesterol-dependent feedback inhibition and that downregulation of both the NPC1 and NPC2 genes/proteins was associated with the sequestration of LDL-derived cholesterol within endocytic compartments, including late endosomes/lysosomes after equilibration. Therefore, it is proposed that physiological and coordinate downregulation of the NPC1 and NPC2 genes/proteins promotes the sequestration of LDL-derived cholesterol within endocytic compartments and serves a role in maintaining intracellular cholesterol homeostasis.

MATERIALS AND METHODS

MATERIALS

DMEM, PBS, trypsin–EDTA, and 100 U/ml penicillin/streptomycin (P/S) for cell culture were purchased from Invitrogen Corporation (Carlsbad, CA). Fetal bovine serum (FBS) and lipoprotein-deficient serum (LPDS) were purchased from Cocalico Laboratories (Reamstown, PA). Complete protease inhibitor cocktail tablets were purchased from Boehringer Mannheim (Indianapolis, IN). Human LDL ($d = 1.019–1.063$) was obtained from the pooled plasma of healthy volunteers and isolated using standard discontinuous density gradient ultracentrifugation. Purified cholesterol, cholesteryl oleate, triacylglycerol, fatty acid-free albumin (FAFA, Fraction V), MES, and Histodenz were purchased from Sigma Chemical Company (St. Louis, MO). The amount of triacylglycerol was determined using Infinity Triacylglycerol Reagent purchased from Thermo Electron Corporation (Pittsburgh, PA). Radiolabeled [^{14}C]-oleate was purchased from General Electric Healthcare (Piscataway, NJ). To extract RNA, the RNeasy Mini Kit and RNase-Free DNase Kit were purchased from Qiagen (Valencia, CA). The TaqMan Gene

Expression Assay, including PCR primers with TaqMan MGB probes (HMG-CoAR, Hs00168352_m1; INSIG-1, Hs01650977_g1; INSIG-2, Hs00379223_m1; LDLR, Hs00181192_m1; NPC1, Hs00264835_m1; NPC2, Hs00197565_m1; SCAP, Hs00378725_m1; SREBP-1, Hs00231674_m1; SREBP-2, Hs00190237_m1) was purchased from Applied Biosystems (Foster City, CA). The NPC1 antibody, generated against amino acids 1254–1273 (NKAKSCATEERYGTERER) of the human NPC1 protein, was custom made and purchased from Invitrogen Corporation. The antibodies for β-actin, Golgi 58K, and NPC2 were purchased from Sigma Chemical Company. The antibodies for LAMP-1 (clone H4A3) and SREBP-2 (sc-8151) were purchased from Santa Cruz Biotechnology (Santa Cruz, CA). The antibodies for SREBP-1 (clone IgG-2A4), SREBP-2 (clone IgG-1C6), and nucleoporin were purchased from BD Biosciences (San Jose, CA). The antibody for PDI (clone RL77) was purchased from Affinity BioReagents (Golden, CO). The antibody for HMG-CoAR was obtained from a hybridoma cell-line (clone IgG-A9) provided by Ta-Yuan Chang (Dartmouth University). The LipidTOX Red neutral lipid stain was purchased from Invitrogen Corporation. Peroxidase, Cy2, and Cy3-conjugated goat secondary antibodies were purchased from Jackson ImmunoResearch Laboratories (West Grove, PA). Polyacrylic acid (50,000 Da) and Aqua Poly/Mount were purchased from Polysciences Incorporated (Warrington, PA). The West Pico SuperSignal Substrate for Western Blotting and Bicinchoninic Acid (BCA) protein assay kits were purchased from Pierce Chemical Company (Rockford, IL).

CELL CULTURE AND HARVEST

Normal human fibroblasts (CRL-2097) were purchased from the American Type Culture Collection (Manassas, VA) and maintained in a humidified incubator at 37°C equilibrated with 5% CO_2 and 95% air. Fibroblasts were maintained and seeded into plates or onto coverslips using DMEM containing 10% fetal bovine serum and 1% penicillin/streptomycin (DMEM, 10% FBS, and 1% P/S). Once the fibroblasts reached ~50% confluence, the media was removed and the cells were rinsed three times with PBS to assure the removal of serum lipoproteins, followed by replacing the media with DMEM containing 5% lipoprotein-deficient serum and 1% penicillin/streptomycin (DMEM, 5% LPDS, and 1% P/S), which depletes cellular sterol pools and increases expression of the LDL receptor. After the fibroblasts reached ~75% confluence (48 h), the media from one set of plates was removed and replaced with fresh media without LDL (DMEM, 5% LPDS, and 1% P/S), while media from a second and third set of plates was removed and replaced with fresh media containing LDL (DMEM, 5% LPDS, 1% P/S, and 50 μg/ml LDL) to allow the endocytosis of LDL (24 h). The fibroblasts contained within the first and second set of plates (denoted as LPDS and LDL-NE, respectively) were later harvested (24 h). However, the media from the third set of plates was removed and the fibroblasts were rinsed three times with PBS containing 2 mg/ml fatty acid-free albumin (PBS and 2 mg/ml FAFA) to assure the absence of LDL, followed by replacing the media with DMEM containing 2 mg/ml fatty acid-free albumin and 1% penicillin/streptomycin (DMEM, 2 mg/ml FAFA, and 1% P/S) to allow the transport of LDL-derived cholesterol from endocytic compartments and equilibration of cellular sterol pools. The fibroblasts contained within the third set of plates (denoted as LDL-E) were later harvested (24 h). For studies described in this report, the fibroblasts grown in media without LDL (LPDS) was considered the basal or control culture condition, while fibroblasts grown in media with LDL and not equilibrated (LDL-NE) or media with LDL and equilibrated (LDL-E) were considered the test culture conditions. For each of these culture conditions, the fibroblasts were harvested for experimentation by either (i) rinsing three times with cold PBS followed by extraction of total lipids using hexane:isopropanol (cholesterol and cholesteryl ester analysis), (ii) rinsing three times with cold PBS followed by extraction of total RNA using the RNeasy Mini Kit (quantitative RT-PCR analysis), (iii) rinsing three times with cold PBS followed by collection of cells with PBS containing protease inhibitors (immunoblot analysis, isolation of plasma membrane and late endosomes/lysosomes), or (iv) removal of media and fixation of cells using PBS containing paraformaldehyde (fluorescence microscopy analysis).

CHOLESTEROL AND CHOLESTERYL ESTER ANALYSIS

To determine the concentration of cholesterol and cholesteryl ester, total lipids were separated using TLC. In brief, the fibroblasts or the isolated plasma membranes were rinsed three times with cold PBS and total lipids were extracted using hexane:isopropanol (3:2, v/v). The organic phase was dried with nitrogen gas and the resulting lipids were resuspended in chloroform and applied onto a silica TLC plate that was developed with hexane:diethyl ether:glacial acetic acid (80:20:1, v/v/v). Cholesterol and cholesteryl ester were identified using standards after staining with iodine vapor. After destaining, the cholesterol and cholesteryl ester were removed from the plate, hydrolyzed using ethanol containing 0.1 M KOH (80°C for 1 h) and extracted using hexane:water (3:1, v/v). A fraction of the resulting hexane phase was collected and dried with nitrogen gas. The amount of cholesterol and cholesteryl ester was determined using the cholesterol oxidase method. The amount of cholesterol and cholesteryl ester was then normalized to the corresponding protein that was precipitated with organic solvent and measured using the BCA method to determine the concentration of cholesterol and cholesteryl ester, respectively.

CHOLESTEROL ESTERIFICATION BY ACAT

To determine the relative amount of cholesterol esterification by ACAT, the fibroblasts were rinsed once with PBS and then incubated with DMEM containing 2.7 μg/ml [^{14}C]-oleate bound to 0.6 mg/ml BSA (37°C for 1 h). After incubation, the cells were rinsed twice with cold PBS containing 1 mg/ml BSA, and then twice with cold PBS. The total lipids were extracted from the cells using hexane:isopropanol (3:2, v/v) and incorporation of the radiolabeled oleate into cholesteryl ester, which represented the amount of cholesterol esterification by ACAT, was determined after separation of the lipids using TLC. The amount of cholesteryl ester was then normalized to the corresponding protein that was precipitated with organic solvent and measured using the BCA method to determine the ACAT activity.

ISOLATION OF THE PLASMA MEMBRANE

The plasma membrane was isolated from human fibroblasts using cationic colloidal silica and polyacrylic acid as previously described

[Garver et al., 2002]. In brief, the cells were rinsed once with cold PBS, and then twice with cold MES buffer (20 mM MES pH 6.5 and 135 mM NaCl). The cells were incubated with cold MES buffer containing 1.0% cationic colloidal silica to coat the plasma membrane (4°C for 10 min), followed by the cells being rinsed once with MES buffer to remove residual cationic colloidal silica. The cells were then incubated with cold MES buffer containing 1.0 mg/ml polyacrylic acid to cross-link the cationic colloidal silica (4°C for 10 min), followed by the cells being rinsed twice with cold MES buffer to remove residual polyacrylic acid. The cells were scraped from the plate with cold MES buffer containing protease inhibitors and pelleted using centrifugation (1,000*g* at 4°C for 10 min). The supernatant was removed and the pelleted cells were resuspended into 1.0 ml hypotonic MES homogenization buffer (20 mM MES pH 6.5, 2.0 mM EDTA, and protease inhibitors), incubated to allow osmosis-induced enlargement of the cells (4°C for 30 min), and then homogenized using a type C Teflon-glass homogenizer. The homogenized sample was diluted with an equal volume of MES buffer containing 100% (w/v) Histodenz resulting in a homogenate that contained 50% (w/v) Histodenz. This mixture was layered onto a 70–55% (w/v) linear Histodenz gradient dissolved in MES buffer followed by centrifugation (60,000*g* at 4°C for 30 min). The purified cationic colloidal silica and polyacrylic acid-coated plasma membrane was recovered from bottom of the tube and rinsed twice with cold MES buffer.

ISOLATION OF LATE ENDOSOMES/LYSOSOMES

The late endosomes/lysosomes were isolated from human fibroblasts using differential and isopycnic sucrose density gradient centrifugation [Gasingirwa et al., 2008]. In brief, cells were rinsed three times with cold PBS, scraped from the plates with cold PBS containing protease inhibitors, and then homogenized with a hypotonic buffer (10 mM Tris pH 8.0, 2 mM EDTA, and protease inhibitors) using a small-clearance 15-ml Dounce homogenizer. Differential centrifugation of the cellular homogenate was performed using slow-speed centrifugation (2,000*g* at 4°C for 9 min) to pellet the nuclei, large cellular fragments, and intact cells (N fraction). The resulting supernatant was collected and the N fraction was re-homogenized and re-centrifuged using the same conditions, followed by combining the two post-nuclear supernatant fractions and medium-speed centrifugation (4,300*g* at 4°C for 7 min) to pellet the heavy mitochondrial fraction (M fraction). Next, the resulting supernatant was subjected to high-speed centrifugation (41,300*g* at 4°C for 7 min) to pellet the light mitochondrial fraction (L fraction). Finally, the M and L fractions (enriched with late endosomes/lysosomes) were resuspended into equal volumes of hypotonic buffer, combined, and layered onto a discontinuous sucrose density gradient consisting of 10 layers (density 1.09–1.26 g/ml), followed by high-speed centrifugation (34,200*g* at 4°C for 150 min) using a SW41Ti Beckman swinging bucket rotor. After centrifugation, ten equivalent fractions and the pellet from each tube were collected and immunoblot analysis was performed to identify fractions enriched with LAMP-1, a marker protein for late endosomes/lysosomes. The fractions that were relatively enriched with LAMP-1 and containing late endosomes/lysosomes tended to sediment at a higher sucrose density than fractions that were relatively deficient of LAMP-1 and containing other endocytic compartments. The fractions relatively enriched with LAMP-1 were combined and the concentration of protein within these samples was determined. Total lipids were extracted from these samples using chloroform:methanol (2:1) after being normalized for equivalent amounts of protein [Folch et al., 1957]. The resulting organic phase was collected and dried with nitrogen gas in preparation for the separation of cholesterol, cholesteryl ester, and triacylglycerol using TLC as described above.

IMMUNOBLOT ANALYSIS

The relative amounts of protein were determined using immunoblot analysis. Protein samples were separated using 6%, 8%, 10%, or 12% SDS–PAGE under reduced conditions and then transferred to a nitrocellulose membrane. In brief, blocking buffer (10 mM sodium phosphate pH 7.4, 150 mM NaCl, 0.05% Tween 20, and 5% non-fat dry milk) was used to block non-specific sites on the nitrocellulose membrane (2 h). The membranes were then incubated in blocking buffer containing the appropriate dilution of primary antibody (4°C for 16 h). The membranes were rinsed with blocking buffer (3 × 10 min) to remove residual primary antibody and then incubated in blocking buffer containing the appropriate dilution of peroxidase-conjugated goat secondary antibody (90 min). The membranes were rinsed with blocking buffer (3 × 10 min) to remove residual secondary antibody and enhanced chemiluminescence (ECL) was performed to obtain autoradiograms. The relative amounts of target protein and endogenous control protein (β-actin) were quantified within the linear range of film using a BioRad Model GS-700 Imaging Densitometer.

FLUORESCENCE LABELING

Fibroblasts were fixed using PBS containing 4% paraformaldehyde (30 min). After fixation, the cells were rinsed with PBS (3 × 5 min) and placed in quenching buffer (PBS and 50 mM NH_4Cl) to deactivate the paraformaldehyde (15 min). The cells were then rinsed again with PBS (3 × 5 min) and incubated with blocking buffer containing filipin (PBS, 10% goat serum, and 0.05% filipin) to stain cholesterol (90 min), or the cells were incubated with a different blocking buffer (PBS, 3.0% FAFA, and 0.05% saponin) in preparation to stain cholesteryl ester (90 min), followed by being rinsed with PBS (3 × 5 min) to remove saponin. The cells were then incubated with respective blocking buffers (PBS, 10% goat serum, and 0.05% filipin, or PBS and 1.0% FAFA) containing the appropriate dilution of primary antibodies (90 min). After the cells were rinsed with PBS (3 × 5 min) to remove residual primary antibody, the cells were incubated with respective blocking buffers containing the appropriate dilution of Cy2 or Cy3-conjugated goat secondary antibodies, or LipidTOX Red neutral lipid stain (90 min). Cells were then rinsed with PBS (3 × 5 min) to remove residual secondary antibody, filipin, and LipidTOX Red neutral lipid stain, followed by mounting the coverslips onto slides using Aqua Poly/Mount.

DECONVOLUTION FLUORESCENCE MICROSCOPY

Deconvolution fluorescence microscopy is a relatively new technique that decreases the amount of unfocused and distorted

fluorescence through computational processing, thereby promoting the restoration of multiple focal planes into a high-resolution three-dimensional image. The images were obtained using an Olympus IX-70 inverted microscope equipped with a 60× (NA 1.4) oil immersion objective (Olympus America, Melville, NY), Photometrics cooled CCD camera (Roper Scientific Instruments, Tucson, AZ), and DeltaVision RT restoration microscopy system software (Applied Precision, Issaquah, WA). The emission wavelengths used for obtaining fluorescent images were 350 nm for the DAPI filter, 528 nm for the Cy2 filter, and 617 nm for the Cy3 filter. For each of the different fluorescent probes, 26 sections were obtained using a distance of 0.2 μm (recommended step size for the NA of the objectives) set between focal planes. The data, subjected to 10 deconvolution iterations, were projected using SoftWoRX software that was processed using identical parameters with Adobe Photoshop software CS2 (Adobe Systems, Mountain View, CA).

RNA PREPARATION

Total RNA was extracted from fibroblasts using the RNeasy Mini Kit including treatment of the RNA with RNase-free DNase to remove any contaminating DNA. The concentration of RNA was determined by absorbance at 260 nm, with the purity of RNA determined by the ratio of absorbance at 260 and 280 nm.

REVERSE TRANSCRIPTION AND QUANTITATIVE RT-PCR

The relative amounts of targeted mRNA were determined using reverse transcription and quantitative RT-PCR analysis. Reverse transcription was performed using 2.5 μM random hexamers, 4.0 mM dNTP's, 15 mM $MgCl_2$, 50 U reverse transcriptase, and 100 U RNA inhibitor to produce the cDNA. Pre-developed commercially available primers and probes were used for detection of the following targets: HMG-CoAR, INSIG-1, INSIG-2, LDLR, NPC1, NPC2, SCAP, SREBP-1, and SREBP-2. The quantitative RT-PCR was performed with a TaqMan Gene Expression Assay containing PCR primers and TaqMan MGB probe (FAM dye-labeled) using an ABI-PRISM Sequence Detection System (Applied Biosystems). The relative quantification of PCR products was normalized to 18S rRNA (internal control).

STATISTICAL ANALYSIS

For all experiments, quantitative data is represented as the mean ± standard deviation (SD) using five plates of cells (cholesterol and cholesteryl ester analysis for the whole cell), three plates of cells (cholesterol analysis for the isolated plasma membrane and quantitative RT-PCR analysis), or one large plate of cells that were processed by performing five separate lipid extractions of the isolated late endosomes/lysosomes (cholesterol, cholesteryl ester, and triacylglycerol analysis) for each of the respective culture conditions. Significant differences ($P \leq 0.05$) between two groups of data were determined using the two-tailed Student's *t*-test assuming equal variance.

RESULTS

CONCENTRATION OF CELLULAR CHOLESTEROL AND CHOLESTERYL ESTER, PLASMA MEMBRANE CHOLESTEROL, AND AMOUNT OF CHOLESTEROL ESTERIFICATION BY ACAT

The concentration of cellular cholesterol and cholesteryl ester, plasma membrane cholesterol, and amount of cholesterol esterification by ACAT were determined in fibroblasts using the three culture conditions (Fig. 1). When fibroblasts were grown with LDL (LDL-NE and LDL-E) the concentration of cellular cholesterol was significantly increased (to 3- and 1.8-fold, respectively) compared to fibroblasts grown in LPDS, which was designated the basal culture condition (Fig. 1A). Moreover, the concentration of cellular cholesteryl ester was significantly increased (to ~25-fold) in fibroblasts grown with LDL (LDL-NE and LDL-E) compared to fibroblasts grown in LPDS. The concentration of cellular cholesterol decreased (to 60%) when fibroblasts were grown with LDL and equilibrated (LDL-E) compared to fibroblasts not equilibrated (LDL-NE), consistent with the transport and redistribution of cholesterol from endocytic compartments to the endoplasmic reticulum for esterification by ACAT (Fig. 1B). The results also indicated a modest but significant increase (to 1.3-fold) in the concentration of plasma membrane cholesterol in fibroblasts grown with LDL and not equilibrated (LDL-NE) compared to fibroblasts grown in LPDS (Fig. 1C). However, when fibroblasts were grown with LDL and equilibrated (LDL-E) the concentration of plasma membrane cholesterol decreased significantly (to 85%), thereby returning to the same approximate concentration of plasma membrane cholesterol as fibroblasts grown in LPDS. It is important to emphasize that the plasma membranes were purified to near homogeneity based on a fivefold increase in the concentration of cholesterol associated with this fraction compared to the concentration of total cellular cholesterol, consistent with the plasma membrane representing a relatively cholesterol-enriched cellular compartment. When fibroblasts were grown with LDL (LDL-NE and LDL-E) ACAT activity was significantly increased (to 5.7- and 4.9-fold, respectively) compared to fibroblasts grown in LPDS (Fig. 1D). Therefore, a significantly increased amount of cellular cholesterol (1.8-fold) that was not associated with the plasma membrane or available for esterification by ACAT remained associated with undefined cellular compartments after fibroblasts were equilibrated.

CONCENTRATION OF CHOLESTEROL, CHOLESTERYL ESTER, AND TRIACYLGLYCEROL ASSOCIATED WITH LATE ENDOSOMES/LYSOSOMES

The concentration of cholesterol, cholesteryl ester, and triacylglycerol associated with late endosomes/lysosomes was determined in fibroblasts using the three culture conditions (Fig. 2). To ascertain the relative purity of late endosomes/lysosomes isolated from these fibroblasts, the relative amount of organelle marker proteins was determined for cellular homogenates and isolated late endosomes/lysosomes using immunoblot analysis (Fig. 2A). The results indicated a drastic enrichment of a marker protein for late endosomes/lysosomes (LAMP-1), in addition to an almost complete absence of other marker proteins for the plasma membrane and

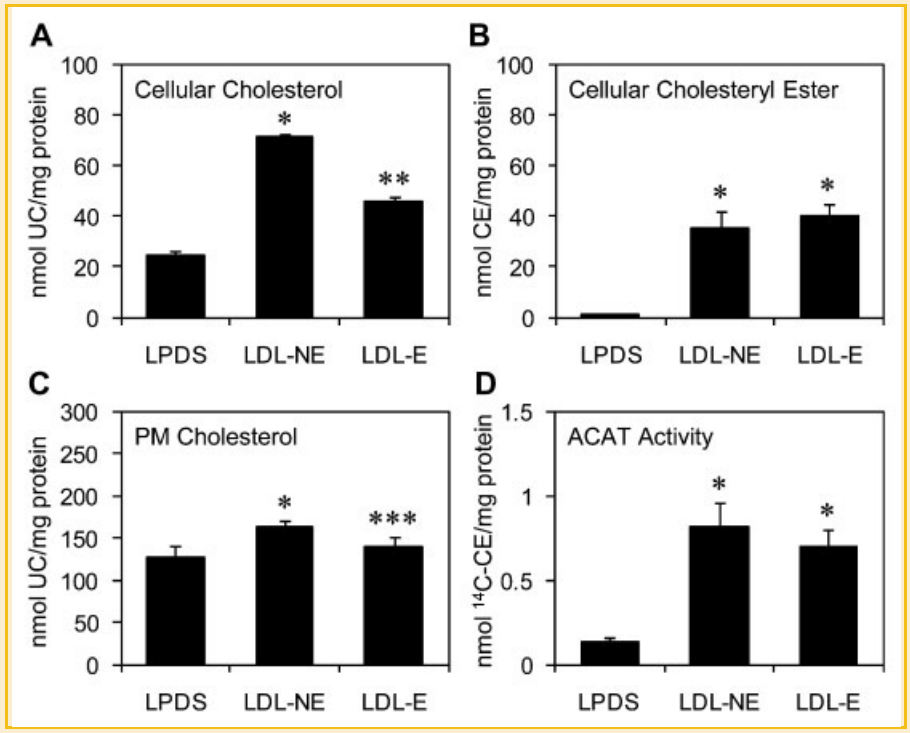

Fig. 1. Concentration of cellular cholesterol and cholesteryl ester, plasma membrane cholesterol, and amount of cholesterol esterification by ACAT. Fibroblasts were grown using the three culture conditions (LPDS, LDL-NE, and LDL-E) and then processed as described in Materials and Methods Section. The amount of cellular cholesterol and cholesteryl ester was normalized to the corresponding cellular protein to provide the concentration of cellular cholesterol (A) and cholesteryl ester (B). After isolation of the plasma membrane, the amount of plasma membrane cholesterol was normalized to the corresponding plasma membrane protein to provide the concentration of plasma membrane (PM) cholesterol (C). The amount of cholesteryl ester produced by ACAT was normalized to the corresponding cellular protein to provide the ACAT activity (D). The values represent the mean ± SD obtained from five plates of fibroblasts. UC = unesterified cholesterol. CE = cholesteryl ester. $^{*}P \leq 0.05$ compared to fibroblasts grown in LPDS. $^{**}P \leq 0.05$ compared to fibroblasts grown in LPDS or LDL-NE. $^{***}P \leq 0.05$ compared to fibroblasts grown in LDL-NE.

cytoskeleton (β-actin), nucleus (nucleoporin), Golgi apparatus (Golgi 58 K protein), and endoplasmic reticulum (PDI) compared to the cellular homogenate. With respect to the concentration of lipids associated with late endosomes/lysosomes isolated from these fibroblasts, the results indicated no significant difference in the concentration of cholesterol for fibroblasts grown with LDL and not equilibrated (LDL-NE) compared to fibroblasts grown in LPDS (Fig. 2B). However, fibroblasts grown with LDL and equilibrated (LDL-E) had a significantly increased concentration (to 1.6-fold) of cholesterol associated with late endosomes/lysosomes compared to fibroblasts grown in LPDS. The concentration of neutral lipids, specifically cholesteryl ester and triacylglycerol, associated with late endosomes/lysosomes were found to be exceedingly low with no significant differences among fibroblasts grown using the three culture conditions. Therefore, although fibroblasts grown with LDL and not equilibrated (LDL-NE) had significantly increased concentrations of cellular cholesterol, the cholesterol was not associated with late endosomes/lysosomes isolated from these fibroblasts. However, fibroblasts grown with LDL and equilibrated (LDL-E), which actually had significantly decreased concentrations of cellular cholesterol, had significantly increased concentrations of cholesterol associated with late endosomes/lysosomes.

DISTRIBUTION OF CELLULAR CHOLESTEROL AND CHOLESTERYL ESTER IN RELATION TO LATE ENDOSOMES/LYSOSOMES

The distribution of cellular cholesterol and cholesteryl ester in relation to the LAMP-1 protein (a marker protein for late endosomes/lysosomes, but also associated with other endocytic compartments) were determined in fibroblasts grown using the three culture conditions. With respect to cellular cholesterol, the images indicated two primary cellular distributions, one represented by the plasma membrane, and the other represented by various perinuclear cytoplasmic vesicles (Fig. 3). When the distribution of cellular cholesterol was examined in relation to the LAMP-1 protein, a population of semi-rounded and hollowed vesicles were relatively cholesterol-enriched in fibroblasts grown with LDL and not equilibrated (LDL-NE) compared to fibroblasts grown in LPDS. Moreover, in fibroblasts grown with LDL and equilibrated (LDL-E), a population of the vesicles was also found to be relatively cholesterol-enriched, indicating that these compartments had the capability of sequestering LDL-derived cholesterol. With respect to cellular cholesteryl ester, the images also indicated two primary cellular distributions, depending on whether the fibroblasts were grown in LPDS or with LDL (LDL-NE and LDL-E; Fig. 4). When the fibroblasts were grown in LPDS, there was only faint staining of cytoplasmic vesicles. In contrast, when the fibroblasts were grown

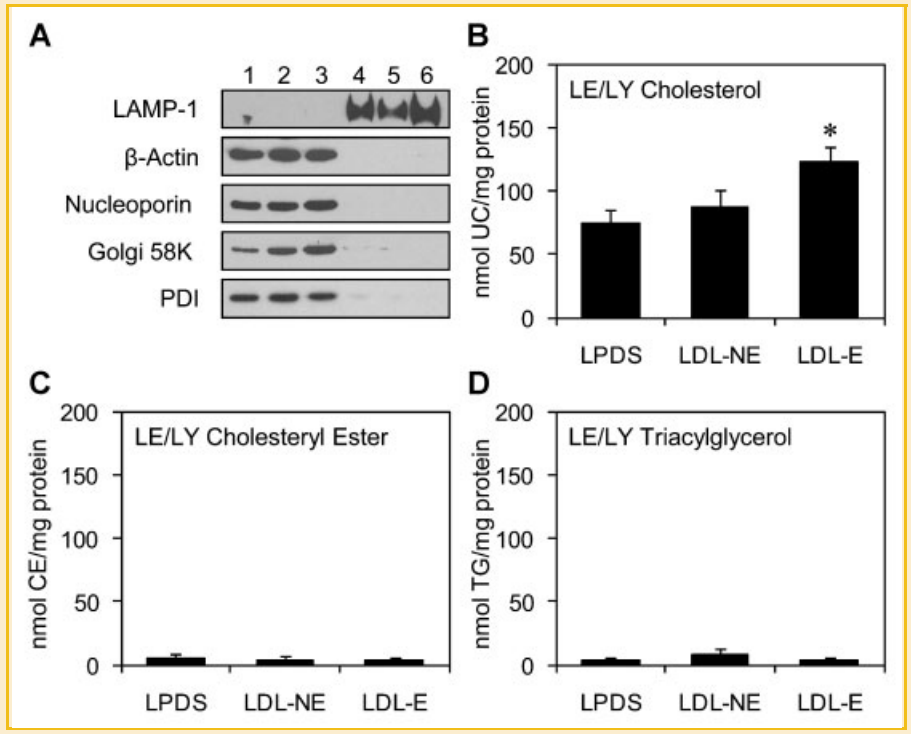

Fig. 2. Concentration of cholesterol, cholesteryl ester, and triacylglycerol associated with late endosomes/lysosomes. Fibroblasts were grown using the three culture conditions (LPDS, LDL-NE, and LDL-E) and then processed as described in Materials and Methods Section. After isolation of the late endosomes/lysosomes, the relative purity of these compartments in comparison to the cellular homogenate was determined using immunoblot analysis with organelle marker proteins (A). The amount of cholesterol, cholesteryl ester, and triacylglycerol associated with late endosomes/lysosomes (LE/LY) was normalized to the corresponding protein to provide the concentration of LE/LY cholesterol (B), LE/LY cholesteryl ester (C), and LE/LY triacylglycerol (D). The values represent the mean ± SD obtained from five independent lipid extractions of the isolated late endosomes/lysosomes obtained from one large plate of cells grown using the three culture conditions. $^{*}P \leq 0.05$ compared to fibroblasts grown in LPDS. UC = unesterified cholesterol. CE = cholesteryl ester. and TG = triacylglycerol. Lane 1, LPDS homogenate; Lane 2, LDL-NE homogenate; Lane 3, LDL-E homogenate; Lane 4, LPDS LE/LY; Lane 5, LDL-NE LE/LY; Lane 6, LDL-E LE/LY.

with LDL, thin-elongated structures present throughout the cytoplasm became enriched with cholesteryl ester. However, neither the cytoplasmic vesicles nor the thin-elongated structures enriched with cholesteryl ester co-localized with the LAMP-1 protein. Therefore, although fibroblasts grown with LDL (LDL-NE and LDL-E) have an increased concentration of cellular cholesteryl ester, there was no detectable co-localization of this lipid with late endosomes/lysosomes. In contrast, late endosomes/lysosomes and other endocytic compartments possibly representing early endosomes/recycling endosomes, were relatively cholesterol-enriched and remained cholesterol-enriched after equilibration, indicating that these compartments sequestered LDL-derived cholesterol.

RELATIVE AMOUNTS OF SREBP-1, SREBP-2, SCAP, AND INSIG-1 mRNA

The relative amounts of SREBP-1, SREBP-2, SCAP, and INSIG-1 mRNA, which encode key proteins representing the SREBP pathway, were determined in fibroblasts grown using the three culture conditions (Fig. 5). The results indicated a significant decrease (to 67% and 56%, respectively) in the relative amounts of SREBP-1 mRNA when fibroblasts were grown with LDL (LDL-NE and LDL-E) compared to the amount of SREBP-1 mRNA in fibroblasts grown in LPDS (Fig. 5A). Similarly, the relative amounts of SREBP-2 mRNA in fibroblasts grown with LDL (LDL-NE and LDL-E) were also significantly decreased (to 14% and 22%, respectively) compared to fibroblasts grown in LPDS (Fig. 5B). With respect to the relative amounts of SCAP mRNA, the results indicated a modest but significant decrease (to 86%) when fibroblasts were grown with LDL and equilibrated (LDL-E) compared to fibroblasts grown in LPDS or with LDL and not equilibrated (Fig. 5C). The relative amounts of INSIG-1 mRNA decreased dramatically (to ~1%) when fibroblasts were grown with LDL (LDL-NE and LDL-E) compared to fibroblasts grown in LPDS (Fig. 5D). In contrast, the relative amounts of INSIG-2 mRNA decreased only modestly (to 80%) when fibroblasts were grown with LDL and equilibrated (LDL-E) compared to fibroblasts grown in LPDS or with LDL and not equilibrated (data not shown). Therefore, the results indicated varying but significant downregulation in the transcription of key genes that encode proteins (SREBP-1, SREBP-2, SCAP, and INSIG-1) representing the SREBP pathway when fibroblasts were grown with LDL.

RELATIVE AMOUNTS OF PRECURSOR AND MATURE SREBP PROTEINS

The relative amounts of precursor (p) and mature (m) SREBP-1 and SREBP-2 proteins was determined in fibroblasts grown using the three culture conditions (Fig. 6). Although the relative amounts of p-SREBP-1 protein were somewhat increased when fibroblasts

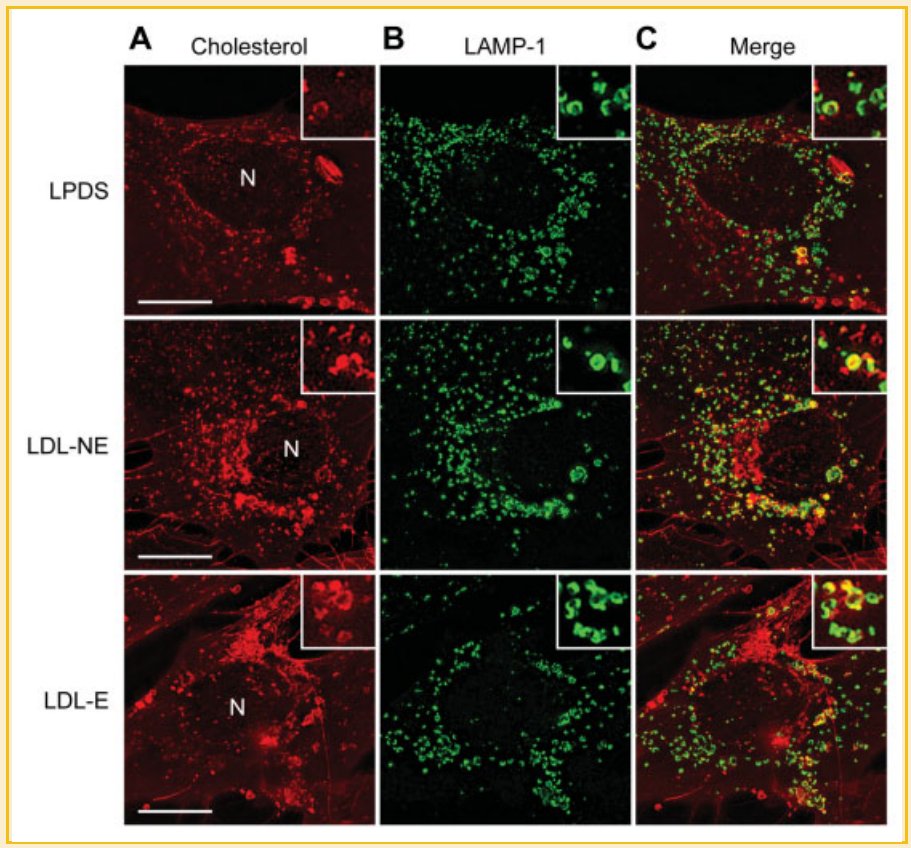

Fig. 3. Distribution of cellular cholesterol in relation to late endosomes/lysosomes. Fibroblasts were grown using the three culture conditions (LPDS, LDL-NE, and LDL-E) and then processed to label cholesterol (A), and the LAMP-1 protein (B), a marker protein for late endosomes/lysosomes. The corresponding merged images were also provided (C). Each image includes an insert of higher magnification (3×). Fluorescent images were obtained using a deconvolution fluorescence microscope equipped with an Olympus 60× (NA 1.4) oil-immersion objective. The single fibroblast provided within each image is representative of other fibroblasts on the same coverslip. All images were acquired and processed using identical conditions. Bar represents 15 μm. N, nucleus.

were grown with LDL (LDL-NE and LDL-E), the differences were not significant compared to fibroblasts grown in LPDS (Fig. 6A). In contrast, the relative amounts of p-SREBP-2 protein for fibroblasts grown with LDL (LDL-NE and LDL-E) were significantly decreased (to 38% and 48%, respectively) compared to fibroblasts grown in LPDS (Fig. 6B). The relative amounts of m-SREBP-1 protein in fibroblasts grown with LDL and not equilibrated (LDL-NE) was significantly decreased (to 36%), and further decreased (to 11%) when fibroblasts were grown in LDL and equilibrated (LDL-E) compared to fibroblasts grown in LPDS (Fig. 6C). Similarly, the relative amounts of m-SREBP-2 protein in fibroblasts grown with LDL (LDL-NE and LDL-E) were significantly decreased (to 11% and 6%, respectively) compared to the amount of m-SREBP-2 protein in fibroblasts grown in LPDS (Fig. 6D). Therefore, the results indicated a major and significant decrease in the production of m-SREBP-1 and m-SREBP-2 proteins when fibroblasts were grown with LDL, consistent with cholesterol-dependent feedback inhibition of the SREBP pathway.

RELATIVE AMOUNTS OF LDLR AND HMG-CoAR mRNA, AND LDLR AND HMG-CoAR PROTEIN

The relative amounts of LDLR and HMG-CoAR mRNA, in addition to the relative amounts of LDLR and HMG-CoAR protein that regulate the endocytosis of LDL and de novo biosynthesis of cholesterol, respectively, were determined in fibroblasts grown using the three culture conditions (Fig. 7). The results indicated a significant decrease (to 8% and 6%, respectively) of LDLR mRNA in fibroblasts grown with LDL (LDL-NE and LDL-E) compared to fibroblasts grown in LPDS (Fig. 7A). Similar to the amount of LDLR mRNA, the relative amounts of HMG-CoAR mRNA decreased significantly (to 12% and 10%, respectively) when fibroblasts were grown with LDL (LDL-NE and LDL-E) compared to fibroblasts grown in LPDS (Fig. 7B). With respect to the encoded LDLR protein, the results indicated a significant decrease (to 15% and 35%, respectively) of the LDLR protein in fibroblasts grown with LDL (LDL-NE and LDL-E) compared to fibroblasts grown in LPDS (Fig. 7C). Similarly, the relative amounts of HMG-CoAR protein decreased significantly (to 3.3% and 1.5%, respectively) when fibroblasts were grown with LDL (LDL-NE and LDL-E) compared to fibroblasts grown in LPDS (Fig. 7D). Therefore, the results indicated a significant decrease in the relative amounts of LDLR and HMG-CoAR mRNA, in addition to the relative amounts of the LDLR and HMG-CoAR protein, consistent with the well-known downregulation of the LDLR and HMG-CoAR genes through feedback inhibition of the SREBP pathway.

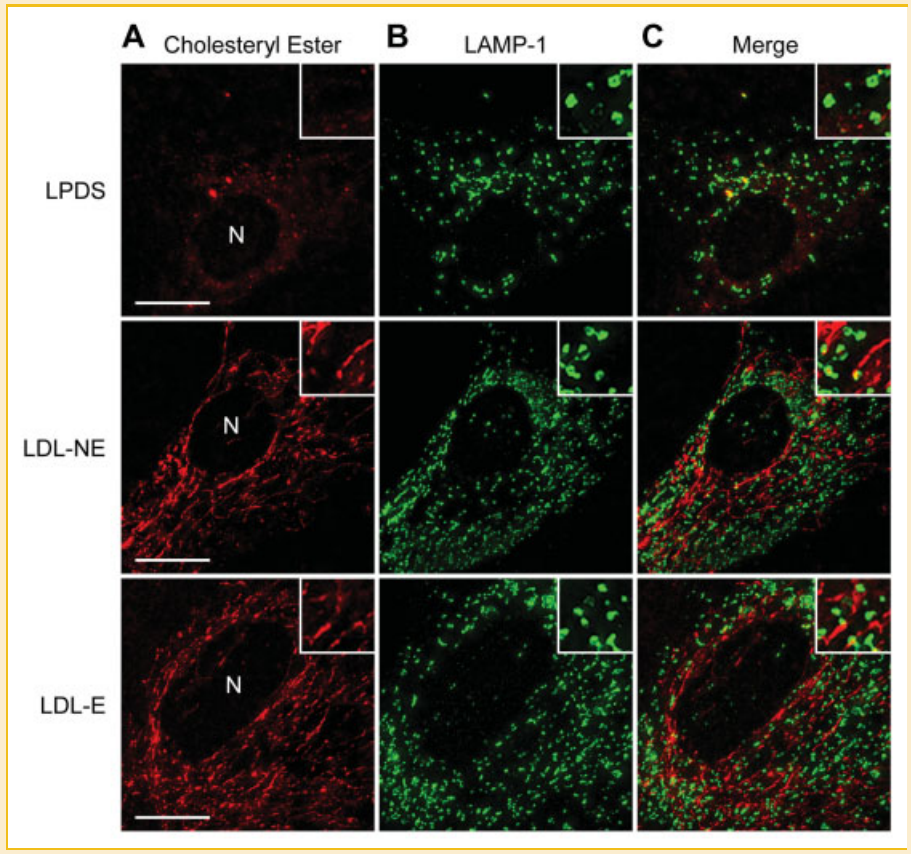

Fig. 4. Distribution of cellular cholesteryl ester in relation to late endosomes/lysosomes. Fibroblasts were grown using the three culture conditions (LPDS, LDL-NE, and LDL-E) and then processed to label cholesteryl ester (A), and the LAMP-1 protein (B), a marker protein for late endosomes/lysosomes. The corresponding merged images were also provided (C). Each image includes an insert of higher magnification (3×). Fluorescent images were obtained using a deconvolution fluorescence microscope equipped with an Olympus 60× (NA 1.4) oil-immersion objective. The single fibroblast provided within each image is representative of other fibroblasts on the same coverslip. All images were acquired and processed using identical conditions. Bar represents 15 μm. N, nucleus.

RELATIVE AMOUNTS OF NPC1 AND NPC2 mRNA, AND NPC1 AND NPC2 PROTEIN

The relative amounts of NPC1 and NPC2 mRNA, in addition to the relative amounts of NPC1 and NPC2 protein that regulate the transport of lipoprotein-derived cholesterol through endocytic compartments, were determined in fibroblasts grown using the three culture conditions (Fig. 8). The results indicated a significant decrease (to 39% and 25%, respectively) of NPC1 mRNA in fibroblasts grown with LDL (LDL-NE and LDL-E) compared to fibroblasts grown in LPDS (Fig. 8A). Similar to the amount of NPC1 mRNA, the relative amounts of NPC2 mRNA decreased significantly (to 58% and 47%, respectively) when fibroblasts were grown with LDL (LDL-NE and LDL-E) compared to fibroblasts grown in LPDS (Fig. 8B). With respect to the encoded NPC1 protein, the results indicated a significant decrease (to 70% and 40%, respectively) of the NPC1 protein in fibroblasts grown with LDL (LDL-NE and LDL-E) compared to fibroblasts grown in LPDS (Fig. 8C). Similarly, the relative amounts of NPC2 protein decreased significantly (to 26% and 23%, respectively) when fibroblasts were grown with LDL (LDL-NE and LDL-E) compared to fibroblasts grown in LPDS (Fig. 8D). Therefore, although the NPC1 gene has already been shown to be downregulated by feedback inhibition by the SREBP pathway, the NPC2 gene is also downregulated by cholesterol-dependent feedback inhibition, although the specific mechanism remains undefined.

DISCUSSION

The present study was performed to determine whether physiological downregulation of the NPC1 gene/protein alters the transport and metabolism of low-density lipoprotein (LDL)-derived cholesterol in human fibroblasts. To perform these studies, fibroblasts were grown in media with LPDS, which represented the basal culture condition, in addition to fibroblasts grown in LPDS supplemented with human LDL that was either not equilibrated (LDL-NE) or equilibrated (LDL-E). The equilibration of fibroblasts was specifically incorporated to allow complete hydrolysis of LDL-derived cholesteryl ester and subsequent transport of cholesterol from the endocytic compartments, in addition to equilibration of cellular sterol pools that included both the ACAT-accessible pool and sterol regulatory pool. In brief, the results indicated that in addition to the NPC1 gene/protein, the NPC2 gene/protein was also downregulated by LDL-derived cholesterol-dependent feedback inhibition and that

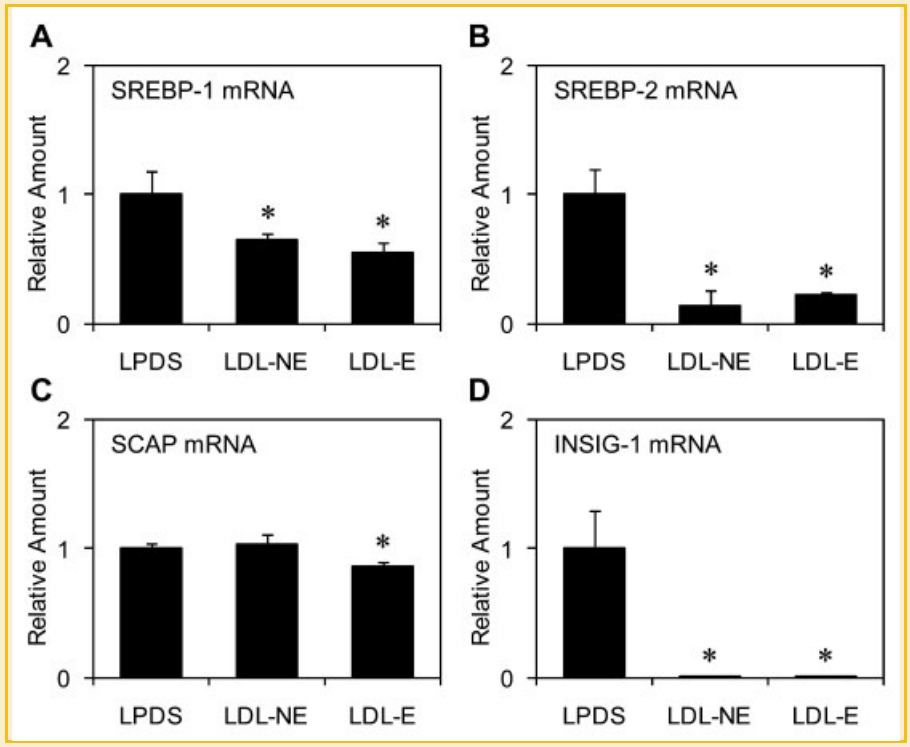

Fig. 5. Relative amounts of SREBP-1, SREBP-2, SCAP, and INSIG-1 mRNA. Fibroblasts were grown using the three culture conditions (LPDS, LDL-NE, and LDL-E) and then processed to perform quantitative RT-PCR. The amounts of SREBP-1, SREBP-2, SCAP, and INSIG-1 mRNA were normalized to the corresponding amounts of 18S rRNA (internal control). The average amounts of SREBP-1 mRNA (A), SREBP-2 mRNA (B), SCAP mRNA (C), and INSIG-1 mRNA (D) for fibroblasts grown in LPDS (designated the basal culture condition) were assigned an arbitrary value of 1.0, while the relative average amounts of SREBP-1 mRNA, SREBP-2 mRNA, SCAP mRNA, and INSIG-1 mRNA for fibroblasts grown with LDL (LDL-NE and LDL-E) were expressed as fold change. $^{*}P \leq 0.05$ compared to fibroblasts grown in LPDS.

downregulation of both the NPC1 and NPC2 genes/proteins was associated with the sequestration of LDL-derived cholesterol within endocytic compartments, including late endosomes/lysosomes after equilibration. Therefore, it is proposed that physiological and coordinate downregulation of the NPC1 and NPC2 genes/proteins promotes the sequestration of LDL-derived cholesterol within endocytic compartments and serves a role in maintaining intracellular cholesterol homeostasis.

The different culture conditions had a significant effect on both the concentration and distribution of cellular cholesterol and cholesteryl ester in fibroblasts. When fibroblasts were grown with LDL and not equilibrated, there was a large increase in the concentration of cellular cholesterol, in addition to a small but significant and transient increase in the concentration of plasma membrane cholesterol. These results would be consistent with the initial hydrolysis of LDL-derived cholesteryl ester, enrichment of cholesterol within endocytic compartments, and the rapid transport of cholesterol to the plasma membrane [Brasaemle and Attie, 1990; Johnson et al., 1990]. Moreover, the resulting increase in both the concentration of plasma membrane cholesterol and cellular cholesteryl ester were consistent with other studies indicating that a portion of the LDL-derived cholesterol first mixes with plasma membrane cholesterol, and that only after expansion beyond a critical threshold level is cholesterol then transported from the plasma membrane to the endoplasmic reticulum for esterification by ACAT [Tabas et al., 1988; Xu and Tabas, 1991]. Interestingly, recent studies have provided a mechanistic explanation for how increased plasma membrane cholesterol promotes internalization and esterification of cholesterol based on the complexation and chemical activity of cholesterol associated with plasma membrane phospholipids [Radhakrishnan and McConnell, 2000; Lange et al., 2004]. However, it must be noted that at least a portion (approximately 30%) of the LDL-derived cholesterol has been shown to be transported from endocytic compartments to the endoplasmic reticulum, independent of the plasma membrane [Neufeld et al., 1996; Underwood et al., 1998].

As anticipated, compared to fibroblasts grown with LDL and not equilibrated, fibroblasts that were grown with LDL and allowed to equilibrate had a significant decrease in both the concentration of cellular and plasma membrane cholesterol, with the concentration of plasma membrane cholesterol returning to the same approximate concentration as fibroblasts that were grown in LPDS. The decrease in the concentration of cellular and plasma membrane cholesterol was paralleled by a significant increase in ACAT activity compared to fibroblasts grown in LPDS, but only a slight and non-significant increase in the concentration of cellular cholesteryl ester compared to fibroblasts grown with LDL and not equilibrated. Moreover, the concentration of cellular cholesterol in fibroblasts grown with LDL and allowed to equilibrate remained significantly increased (1.8-fold) compared to fibroblasts grown in LPDS, consistent with

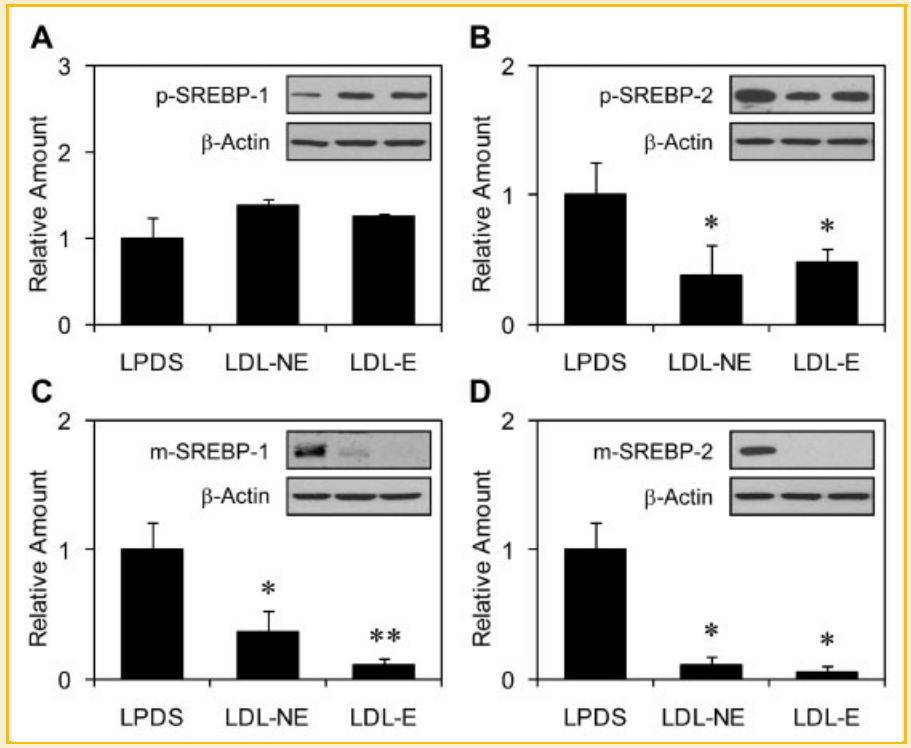

Fig. 6. Relative amounts of precursor and mature SREBP protein. Fibroblasts were grown using the three culture conditions (LPDS, LDL-NE, and LDL-E) and then processed to perform immunoblot analysis. The amounts of p-SREBP-1, p-SREBP-2, m-SREBP-1, and m-SREBP-2 protein were normalized to the corresponding amounts of β-actin (internal control). The average amounts of p-SREBP-1 protein (A), p-SREBP-2 protein (B), m-SREBP-1 protein (C), and m-SREBP-2 protein (D) for fibroblasts grown in LPDS (designated the basal culture condition) were assigned an arbitrary value of 1.0, while the relative average amounts of p-SREBP-1 protein, p-SREBP-2 protein, m-SREBP-1 protein, and m-SREBP-2 protein for fibroblasts grown with LDL (LDL-NE and LDL-E) were expressed as fold change. A representative immunoblot for the respective proteins was incorporated into graphs. $^{*}P \leq 0.05$ compared to fibroblasts grown in LPDS. $^{**}P \leq 0.05$ compared to fibroblasts grown in LDL-NE.

the sequestration of LDL-derived cholesterol within endocytic compartments. Importantly, the concentration of cholesterol associated with late endosomes/lysosomes isolated from fibroblasts grown with LDL and equilibrated was significantly increased (1.6-fold) compared to fibroblasts grown in LPDS, therefore suggesting that endocytic compartments other than late endosomes/lysosomes also sequestered LDL-derived cholesterol. It is proposed that these other endocytic compartments may represent early endosomes/recycling endosomes, based on cholesterol content and putative role in regulating intracellular cholesterol transport to the plasma membrane [Hornick et al., 1997; Mondal et al., 2009].

A significant increase in the concentration of cellular cholesterol when fibroblasts were grown with LDL was consistent with enhanced filipin-staining of various cytoplasmic vesicles present within the perinuclear region of these cells. The images indicated that LAMP-1 containing vesicles, primarily represented by late endosomes/lysosomes but also most likely other endosomal compartments, became relatively cholesterol-enriched when fibroblasts were grown in the presence of LDL compared to fibroblasts grown in LPDS. It is important to emphasize that recent studies have demonstrated that the NPC1 protein is capable of regulating the transport of LDL-derived cholesterol from distinct acidic compartments, residing between early and late endosomes, directly to the *trans*-Golgi network [Sugii et al., 2003; Urano et al., 2008]. Whether the sequestration of LDL-derived cholesterol is occurring in early, intermediate, or late endosomes/lysosomes, it is interesting to note that studies performed using human NPC1 heterozygous fibroblasts, which express approximately one-half the normal amounts of functional NPC1 protein, have also been shown to sequester intermediate amounts of LDL-derived cholesterol within undefined endocytic compartments [Kruth et al., 1986; Garver et al., 2002]. Therefore, whether NPC1 protein function is decreased due to genetic mutation or physiological downregulation by feedback inhibition through the SREBP pathway, the cellular and biochemical phenotype is similar and characterized by the sequestration of LDL-derived cholesterol within endocytic compartments.

A number of studies performed in vitro using cultured cells have determined a reduced transcription of SREBP-1a and SREBP-2 genes when the concentration of cellular cholesterol increases, thereby indicating that transcription of these genes are down-regulated by cholesterol-dependent feedback inhibition [Sato et al., 1996; Shimomura et al., 1997]. The mechanism involves excess cholesterol and oxysterol binding to SCAP and INSIG, respectively, to inhibit translocation and processing of p-SREBP proteins to produce m-SREBP proteins [Radhakrishnan et al., 2004, 2007]. Consistent with these results, the present study indicated that the relative amounts of SREBP-1 and SREBP-2 mRNA, in addition to the relative amounts of m-SREBP-1 and m-SREBP-2 protein, were decreased when fibroblasts were grown with LDL, whether or not the fibroblasts were equilibrated, indicating that the transport of

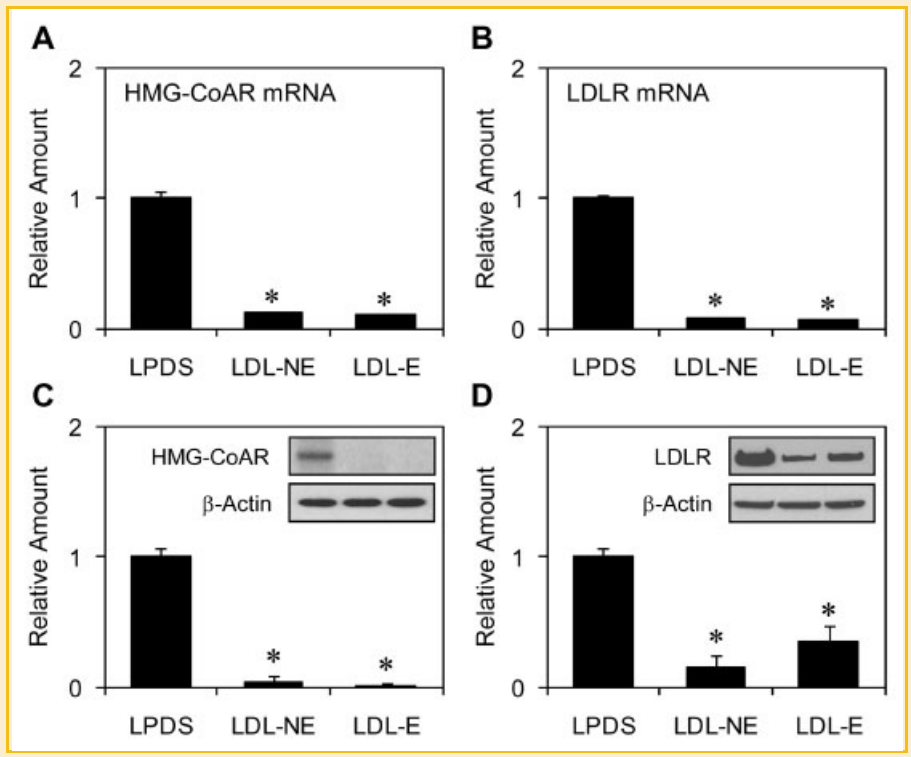

Fig. 7. Relative amounts of LDLR and HMG-CoAR mRNA, and LDLR and HMG-CoAR protein. Fibroblasts were grown using the three culture conditions (LPDS, LDL-NE, and LDL-E) and then processed to perform quantitative RT-PCR and immunoblot analysis. The amounts of LDLR and HMG-CoAR mRNA were normalized to the corresponding amounts of 18S rRNA (internal control), while the amounts of LDLR and HMG-CoAR protein were normalized to the corresponding amounts of β-actin (internal control). The average amounts of LDLR mRNA (A), HMG-CoAR mRNA (B), LDLR protein (C), and HMG-CoAR protein (D) for fibroblasts grown in LPDS (designated the basal culture condition) were assigned an arbitrary value of 1.0, while the relative average amounts of LDLR mRNA, HMG-CoAR mRNA, LDLR protein, and HMG-CoAR protein for fibroblasts grown with LDL (LDL-NE and LDL-E) were expressed as fold change. A representative immunoblot for the respective proteins was incorporated into graphs. $^{*}P \leq 0.05$ compared to fibroblasts grown in LPDS. $^{**}P \leq 0.05$ compared to fibroblasts grown in LDL-NE.

LDL-derived cholesterol to the sterol regulatory pool was rapid and sustainable in promoting feedback inhibition of the SREBP pathway. Moreover, while the relative amount of INSIG-1 mRNA decreased dramatically (to ~1%) when fibroblasts were grown with LDL, the relative amount of INSIG-2 mRNA decreased only modestly (to 80%) when fibroblasts were grown with LDL and equilibrated (data not shown), consistent with downregulation of the INSIG-1 gene, but not the INSIG-2 gene, by the SREBP pathway [Yabe et al., 2002; Yang et al., 2002]. It must be emphasized that both the SREBP-1a and SREBP-2 genes are transcriptionally regulated in a cholesterol-dependent and coordinated-manner in cultured cells, and that both the m-SREBP-1a and m-SREBP-2 proteins are therefore capable of transactivating genes containing either classic sterol regulatory element (SRE-1 and SRE-3) sequences or sterol regulatory element-like (SRE-like) sequences [Amemiya-Kudo et al., 2002]. As a result, with respect to the present study using fibroblasts, both the m-SREBP-1a and m-SREBP-2 proteins were likely responsible for regulating transcription of the SREBP-1, SREBP-2, INSIG-1, and NPC1 genes.

The exact nature of different sterol pools associated with the endoplasmic reticulum involved in either the esterification of excess cellular cholesterol by ACAT or intracellular cholesterol homeostasis by the SREBP pathway remains undefined and controversial [Edwards and Ericsson, 1999]. One study has indicated that a significant fraction of ACAT is enriched with membranes representing a subcompartment of the endoplasmic reticulum that resides in close proximity to the *trans*-Golgi network and endocytic recycling compartment, while another study has suggested that membrane cholesteryl ester generated by ACAT may serve to modulate regulation of the SREBP pathway [Khelef et al., 2000; Iddon et al., 2001]. More recent studies have suggested that the ACAT-accessible pool and sterol regulatory pool are distinct and dissociable, since the transport of LDL-derived cholesterol to the ACAT-accessible pool is relatively delayed [Du et al., 2004; Kristiana et al., 2008]. With respect to the present study, the results indicated maximal esterification of LDL-derived cholesterol and feedback inhibition of the SREBP pathway, and therefore additional studies will be required to determine whether physiological and coordinate downregulation of the NPC1 and NPC2 genes/proteins may alter the transport of cholesterol to the ACAT-accessible pool and sterol regulatory pool.

In summary, the results indicated that in addition to the NPC1 gene/protein, the NPC2 gene/protein was also downregulated by LDL-derived cholesterol-dependent feedback inhibition and that downregulation of both the NPC1 and NPC2 genes/proteins was associated with the sequestration of LDL-derived cholesterol within

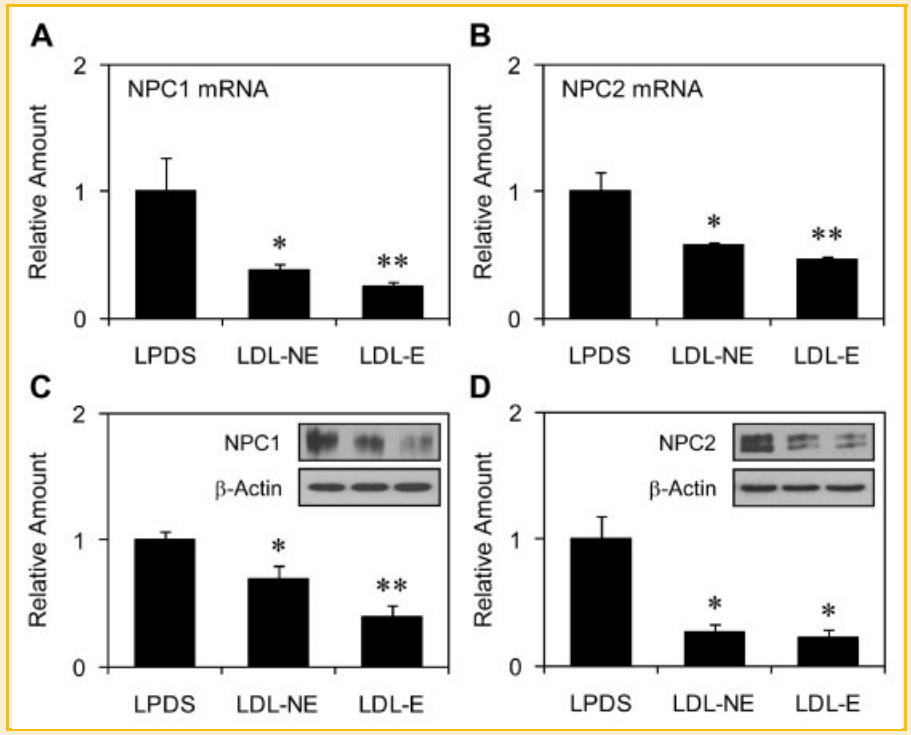

Fig. 8. Relative amounts of NPC1 and NPC2 mRNA, and NPC1 and NPC2 protein. Fibroblasts were grown using the three culture conditions (LPDS, LDL-NE, and LDL-E) and then processed to perform quantitative RT-PCR and immunoblot analysis. The amounts of NPC1 and NPC2 mRNA were normalized to the corresponding amounts of 18S rRNA (internal control), while the amounts of NPC1 and NPC2 protein were normalized to the corresponding amounts of β-actin (internal control). The average amounts of NPC1 mRNA (A), NPC2 mRNA (B), NPC1 protein (C), and NPC2 protein (D) for fibroblasts grown in LPDS (designated the basal culture condition) were assigned an arbitrary value of 1.0, while the relative average amounts of NPC1 mRNA, NPC2 mRNA, NPC1 protein, and NPC2 protein for fibroblasts grown with LDL (LDL-NE and LDL-E) were expressed as fold change. A representative immunoblot for the respective proteins was incorporated into graphs. $^{*}P \leq 0.05$ compared to fibroblasts grown in LPDS. $^{**}P \leq 0.05$ compared to fibroblasts grown in LDL-NE.

endocytic compartments, including late endosomes/lysosomes after equilibration. Therefore, it is proposed that physiological and coordinate downregulation of the NPC1 and NPC2 genes/proteins promotes the sequestration of LDL-derived cholesterol within endocytic compartments and serves a role in maintaining intracellular cholesterol homeostasis.. Although speculative, the physiological and coordinate downregulation of the NPC1 and NPC2 genes/proteins and subsequent sequestration of LDL-derived cholesterol within endocytic compartments provides the first plausible explanation for the accumulation of cholesterol within cells of the artery wall that occurs during atherogenesis.

ACKNOWLEDGMENTS

This work was supported by a National Institutes of Health grant R21-DK071544, a grant from the Tohono O'odham Nation, a grant from the Father's Day Council of Tucson, and other private donations (to W.S.G.), and the Canadian Institutes of Health Research Grant MOP-79532 (to G.A.F.). The authors would also like to express their appreciation to Peter Lobel (Department of Pharmacology, Rutgers University) for sharing expertise concerning the isolation and characterization of late endosomes/lysosomes from cultured cells, and Ta-Yuan Chang (Department of Biochemistry, Dartmouth Medical School) for providing helpful insight and discussion.

REFERENCES

Amemiya-Kudo M, Shimano H, Hasty AH, Yahagi N, Yoshikawa T, Matsuzaka T, Okazaki H, Tamura Y, Iizuka Y, Ohashi K, Osuga J, Harada K, Gotoda T, Sato R, Kumura S, Ishibashi S, Yamada N. 2002. Transcriptional activities of nuclear SREBP-1a, -1c, and -2 to different target promoters of lipogenic and cholesterogenic genes. J Lipid Res 43:1220–1235.

Brasaemle DI, Attie AD. 1990. Rapid intracellular transport of LDL-derived cholesterol to the plasma membrane in cultured fibroblasts. J Lipid Res 31: 103–112.

Brown MS, Goldstein JL. 1986. A receptor-mediated pathway for cholesterol homeostasis. Science 232:34–47.

Brown MS, Goldstein JL. 1997. The SREBP pathway: Regulation of cholesterol metabolism by proteolysis of a membrane-bound transcription factor. Cell 89:331–340.

Carstea ED, Morris JA, Coleman KG, Loftus SK, Zhang D, Cummings C, Gu J, Rosenfeld MA, Pavan WJ, Krizman DB, Nagle J, Polymeropoulos MH, Sturley SL, Ioannou YA, Higgins ME, Comly M, Cooney A, Brown A, Kaneski CR, Blanchette-Mackie EJ, Dwyer NK, Neufeld EB, Chang TY, Liscum L, Tagle DA, Strauss JF III, Ohno K, Zeigler M, Carmi R, Sokol J, Markie D, O'Neill RR, van Diggelen OP, Elleder M, Patterson MC, Brady RO, Vanier MT, Pentchev PG, Tagle DA. 1997. Niemann-Pick C1 disease gene: Homology to mediators of cholesterol homeostasis. Science 277:228–231.

Cheruku SR, Xu Z, Dutia R, Lobel P, Storch J. 2006. Mechanism of cholesterol transfer from the Niemann-Pick type C2 protein to model membranes supports a role in lysosomal cholesterol transport. J Biol Chem 281: 31594–31604.

Du X, Pham YH, Brown AJ. 2004. Effects of 25-hydroxycholesterol on cholesterol esterification and sterol regulatory element binding protein processing are dissociable. J Biol Chem 279:47010–47016.

Edwards PA, Ericsson J. 1999. Sterols and isoprenoids: Signaling molecules derived from the cholesterol biosynthetic pathway. Annu Rev Biochem 68: 157–185.

Folch J, Lees M, Stanley GH. 1957. A simple method for the isolation and purification of total lipids from animal tissues. J Biol Chem 226:497–509.

Friedland N, Liou H-L, Lobel P, Stock AM. 2003. Structure of a cholesterol-binding protein deficient in Niemann-Pick type C2 disease. Proc Natl Acad Sci USA 100:2512–2517.

Garver WS, Heidenreich RA, Erickson RP, Thomas MA, Wilson JM. 2000. Localization of the murine Niemann-Pick C1 protein to two distinct intracellular compartments. J Lipid Res 41:673–687.

Garver WS, Krishnan K, Gallagos JR, Michikawa M, Francis GA, Heidenreich RA. 2002. Niemann-Pick C1 protein regulates cholesterol transport to the *trans*-Golgi network and plasma membrane caveolae. J Lipid Res 43:579–589.

Garver WS, Jelinek D, Francis GA, Murphy BD. 2008. The Niemann-Pick C1 gene is downregulated by feedback inhibition of the SREBP pathway in human fibroblasts. J Lipid Res 49:1090–1102.

Gasingirwa MC, Thirion J, Costa C, Flamion B, Lobel P, Jadot M. 2008. A method to assess the lysosomal residence of proteins in cultured cells. Anal Biochem 374:31–40.

Gevry N, Schoonjans K, Guay F, Murphy BD. 2008. Cholesterol supply and SREBPs modulate transcription of the Niemann-Pick C1 gene in steroidogenic tissues. J Lipid Res 49:1024–1033.

Hornick CA, Hui DY, DeLamatre JG. 1997. A role for retrosomes in intracellular cholesterol transport from endosomes to the plasma membrane. Am J Phys Cell Physiol 273:C1075–C1081.

Iddon CR, Wilkinson J, Bennett AJ, Bennett J, Salter AM, Higgins JA. 2001. A role for smooth endoplasmic reticulum membrane cholesterol ester in determining the intracellular location and regulation of sterol regulatory element binding protein-2. Biochem J 358:415–422.

Infante RE, Abi-Mosleh L, Radhakrishnan A, Dale JD, Brown MS, Goldstein JL. 2008a. Purified NPC1 Protein. I. Binding of cholesterol and oxysterol to a 1278-amino acid membrane protein. J Biol Chem 283:1052–1063.

Infante RE, Radhakrishnan A, Abi-Mosleh L, Kinch LN, Wang ML, Grishin NV, Goldstein JL, Brown MS. 2008b. Purified NPC1 Protein. II. Localization of sterol binding to a 240-amino acid soluble luminal loop. J Biol Chem 283: 1064–1075.

Infante RE, Wang ML, Radhakrishnan A, Kwon HJ, Brown MS, Goldstein JL. 2008c. NPC2 facilitates bidirectional transfer of cholesterol between NPC1 and lipid bilayers, a step in cholesterol egress from lysosomes. Proc Natl Acad Sci USA 105:15287–15292.

Johnson WJ, Chacko GK, Phillips MC, Rothblat GH. 1990. The efflux of lysosomal cholesterol from cells. J Biol Chem 265:5546–5553.

Khelef N, Soe TT, Quehenberger O, Beatini N, Tabas I, Maxfield FR. 2000. Enrichment of acyl coenzyme A:cholesterol acyltransferase near *trans*-Golgi network and endocytic recycling compartment. Arterioscler Thromb 20: 1769–1776.

Ko DC, Binkley J, Sidow A, Scott MP. 2003. The integrity of a cholesterol-binding pocket in Niemann-Pick C2 protein is necessary to control lysosome cholesterol levels. Proc Natl Acad Sci USA 100:2518–2525.

Kristiana I, Yang H, Brown AJ. 2008. Different kinetics of cholesterol delivery to components of the cholesterol homeostatic machinary: Implications for cholesterol trafficking to the endoplasmic reticulum. Biochim Biophys Acta 1781:724–730.

Kruth HS, Comly ME, Butler JD, Vanier MT, Fink JK, Wenger DA, Patel S, Pentchev PG. 1986. Type C Niemann-Pick disease. Abnormal metabolism of low-density lipoprotein in homozygous and heterozygous fibroblasts. J Biol Chem 261:16769–16774.

Lange Y, Ye J, Rigney M, Steck TL. 1999. Regulation of endoplasmic reticulum cholesterol by plasma membrane cholesterol. J Lipid Res 40: 2264–2270.

Lange Y, Ye J, Steck TL. 2004. How cholesterol homeostasis is regulated by plasma membrane cholesterol in excess of phospholipids. Proc Natl Acad Sci USA 101:11664–11667.

Liu R, Lu P, Chu JWK, Sharom FJ. 2009. Characterization of fluorescent sterol binding to purified human NPC1. J Biol Chem 284:1840–1852.

Mondal M, Mesmin B, Mukherjee S, Maxfield FR. 2009. Sterols are mainly in the cytoplasmic leaflet of the plasma membrane and the endocytic recycling compartment in CHO cells. Mol Biol Cell 20:581–588.

Nakamura Y, Takayama N, Minamitani T, Ikuta T, Ariga H, Matsumoto K. 2000. Primary structure, genomic organization and expression of the major secretory protein of murine epididymis, HE1. Gene 251:55–62.

Naureckiene S, Sleat DE, Lackland H, Fensom A, Vanier MT, Wattiaux R, Jadot M, Lobel P. 2000. Identification of HE1 as the second gene of Niemann-Pick C disease. Science 290:2298–2301.

Neufeld EB, Cooney AM, Pitha J, Dawidowicz EA, Dwyer NK, Pentchev PG, Blanchette-Mackie EJ. 1996. Intracellular trafficking of cholesterol monitored with a cyclodextrin. J Biol Chem 271:21604–21613.

Neufeld EB, Wastney M, Patel S, Suresh S, Conney AM, Dwyer NK, Roff CF, Ohno K, Morris JA, Carstea ED, Incardona JP, Strauss JF III, Vanier MT, Patterson MC, Brady RO, Pentchev PG, Blanchette-Mackie EJ. 1999. The Niemann-Pick C1 protein resides in a vesicular compartment linked to retrograde transport of multiple lysosomal cargo. J Biol Chem 274:9627–9635.

Nohturfft A, Yabe D, Goldstein JL, Brown MS, Espenshade PJ. 2000. Regulated step in cholesterol feedback localized to budding of SCAP from ER membranes. Cell 102:315–323.

Ohgami N, Ko DC, Thomas M, Scott MP, Chang CCY, Chang TY. 2004. Binding between the Niemann-Pick C1 protein and a photoactivatable cholesterol analog requires a functional sterol-sensing domain. Proc Natl Acad Sci USA 101:12473–12478.

Radhakrishnan A, McConnell HM. 2000. Chemical activity of cholesterol in membranes. Biochemistry 39:8119–8124.

Radhakrishnan A, Sun LP, Kwon HJ, Brown MS, Goldstein JL. 2004. Direct binding of cholesterol to the purified membrane region of SCAP: Mechanism for a sterol-sensing domain. Mol Cell 15:259–268.

Radhakrishnan A, Ikeda Y, Joo Kwon H, Brown MS, Goldstein JL. 2007. Sterol-regulated transport of SREBPs from endoplasmic reticulum to Golgi: Oxysterols block transport by binding to Insig. Proc Natl Acad Sci USA 104: 6511–6518.

Sato R, Inoue J, Kawabe Y, Kodama T, Takano T, Maeda M. 1996. Sterol-dependent transcriptional regulation of sterol regulatory element binding protein-2. J Biol Chem 271:26461–26464.

Shimomura I, Shimano JD, Horton JD, Goldstein JL, Brown MS. 1997. Differential expression of exons 1a and 1c in mRNAs for sterol regulatory element binding protein-1 in human and mouse organs and cultured cells. J Clin Invest 99:838–845.

Sleat DE, Wiseman JA, El-Banna M, Price SM, Verot L, Shen MM, Tint GS, Vanier MT, Walkley SU, Lobel P. 2004. Genetic evidence for nonredundant functional cooperativity between NPC1 and NPC2 in lipid transport. Proc Natl Acad Sci USA 101:5886–5891.

Sugii S, Reid PC, Ohgami N, Du H, Chang TY. 2003. Distinct endosomal compartments in early trafficking of low-density lipoprotein-derived cholesterol. J Biol Chem 278:27180–27189.

Tabas I, Rosoff WJ, Boykow GC. 1988. Acyl coenzyme A:cholesterol acyltransferase in macrophages utilizes a cellular pool of cholesterol oxidase-accessible cholesterol as substrate. J Biol Chem 263:1266–1272.

Underwood KW, Jacobs NL, Howley A, Liscum L. 1998. Evidence for a cholesterol transport pathway from lysosomes to endoplasmic reticulum that is independent of the plasma membrane. J Biol Chem 273:4266–4274.

Urano Y, Watanabe H, Murphy SR, Shibuya Y, Geng Y, Peden AA, Chang CCY, Chang TY. 2008. Transport of LDL-derived cholesterol from the NPC1 compartment to the ER involves the trans-Golgi network and the SNARE protein complex. Proc Natl Acad Sci USA 105:16513–16518.

Wojtanik KM, Liscum L. 2003. The transport of low-density lipoprotein-derived cholesterol to the plasma membrane is defective in NPC1 cells. J Biol Chem 278:14850–14856.

Xu XX, Tabas I. 1991. Lipoproteins activate acyl-coenzyme A:cholesterol acyltransferase in macrophages only after cellular cholesterol pools are expanded to a critical threshold level. J Biol Chem 266:17040–17048.

Yabe D, Brown MS, Goldstein JL. 2002. Insig-2, a second endoplasmic reticulum protein that binds SCAP and blocks export of sterol regulatory element binding proteins. Proc Natl Acad Sci USA 99:12753–12758.

Yang T, Espenshade PJ, Wright ME, Yabe D, Gong Y, Aebersold R, Goldstein JL, Brown MS. 2002. Crucial step in cholesterol homeostasis: Sterols promote binding of SCAP to Insig-1, a membrane protein that facilitates retention of SREBPs in ER. Cell 110:489–500.